6.3 SEA BREEZE CIRCULATIONS INFLUENCING RADIO FREQUENCY SYSTEM PERFORMANCE AROUND CALIFORNIA BAJA SUR

Robert E. Marshall *
Naval Surface Warfare Center, Dahlgren, Virginia

1. INTRODUCTION

Non-standard radio frequency (RF) propagation in the littorals may enhance or deteriorate the performance of communication and radar systems. Exploiting and ameliorating these four dimensional (4D) effects have long been goals of RF engineers designing systems operating near the coast. Near surface RF propagation is determined by the vertical gradients of temperature and humidity in the coastal atmospheric boundary layer (ABL). Traditionally, RF engineers have relied on a single sounding or a series of helicopter soundings along a single radial to provide a representation of the propagation environment. Recently the 4D aspects of RF system performance have been demonstrated by employing mesoscale numerical weather prediction (NWP) data to drive RF system performance models (Marshall and Haack, 2007). These mesoscale NWP models capture the circulations creating the coastal ABL and thus provide a 4D refractivity field.

2. RADIO REFRACTIVITY

Modified refractivity (M) is employed by RF engineers to describe the propagation characteristics of the atmosphere and is a function of temperature (T), atmospheric pressure (P), vapor pressure (e) and height (z) as shown in 1 (Bean and Dutton, 1966).

$$M = \left(\frac{77.6}{T}\right)\left(P + \frac{4810e}{T}\right) + 0.157z \qquad (1)$$

After substituting the parcel conserved thermodynamic variables, potential temperature (θ) and water vapor mixing ratio (w) for temperature and water vapor pressure respectively it can be shown that near the surface,

$$\frac{dM}{dz} \approx 0.128 + c_1\frac{dw}{dz} - c_2\frac{d\theta}{dz} \qquad (2)$$

The RF propagation environment is categorized by the ranges delineated in Table 1. Sub-refraction directs energy away from the surface and decreases RF range. Super-refraction directs energy along the curvature of the earth and extends RF range. Ducting traps energy between the top of the ABL and the surface and produces blind spots and excessively high radar sea clutter.

* Corresponding *author address:* Robert E. Marshall, *Q41 NSWCDD, 18444 FRONTAGE ROAD SUITE 330 DAHLGREN VA 22448-5161*; Robert.e.marshall@navy.mil.

Behavior	Range 1	Range 2
Standard	= 0.118	
Ducting	< 0.0	
Super-refractive	0.0	0.079
Normal	0.079	0.157
Sub-refractive		> 0.157

Table 1: RF propagation categories in terms of the vertical gradient of modified refractivity.

3. DATA

Figure 1 depicts a three day US Navy vessel cruise off the California Baja Sur in June of 2005. Twelve high vertical resolution meteorological ABL rocketsonde soundings were performed from the vessel during the cruise.

Figure 1: Depiction of a three day US Navy vessel cruise along the California Baja Sur.

The Regional Atmospheric Modeling System (RAMS) was employed to model the mesoscale meteorological structure during the cruise (Marshall, Rottier, Titlow and Bell, 2006). The three nested grids ranged from 36km to 2km over the sounding locations. Figures 2 and 3 display comparisons between RAMS and sounding data at 1822UTC on June 29, 2005. The profile comparison for θ in figure 2 demonstrates that RAMS underestimates the mixed layer height. The profile comparison for w in figure 3 illustrates a

reoccurring NWP difficulty along the west coast of the US during the seasonal northwest Pacific high synoptic circulation. Mesoscale NWP and sounding data comparisons during this cruise and during cruises in the California Bight during this season seem to indicate that the lateral boundary conditions do not contain the widespread dry air captured in the sounding data.

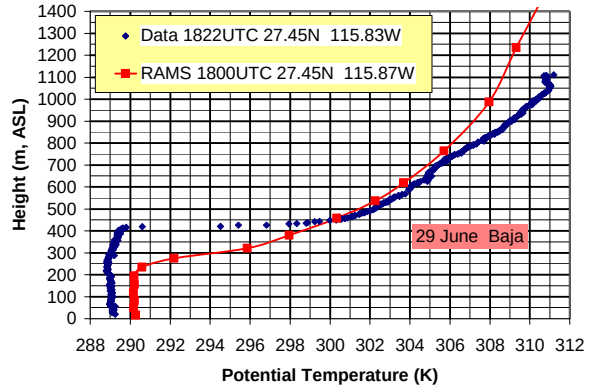

Figure 2: Comparison between sounding and RAMS potential temperature data at 1822UTC on 29 June.

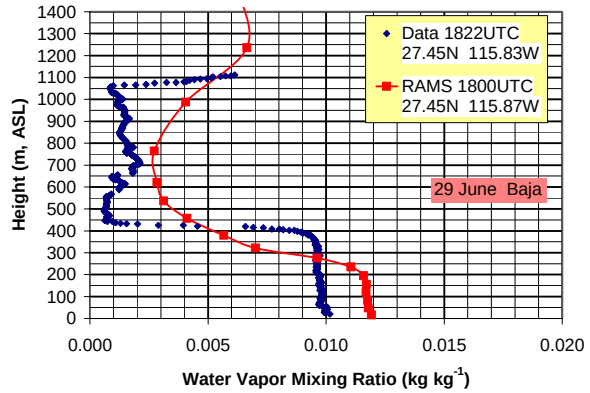

Figure 3: Comparison between sounding and RAMS water vapor mixing ratio data at 1822UTC on 29 June.

The comparisons between the resulting profiles of M are presented in figure 4.

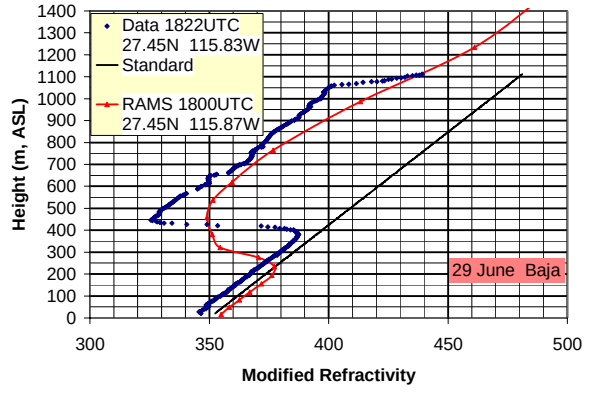

Figure 4: Comparison between sounding and RAMS modified refractivity calculations at 1822UTC on 29 June.

It can be seen in figures 2-4 and equation 2 that the entrainment layer is a breeding ground for RF ducts. This is especially the case if the free atmosphere is significantly less humid than the ABL. For a surface based radar within the ABL, the significance of the duct is that transmitted energy may not escape the entrainment layer at low incident angles leaving a radar "hole" in the lowest layer of the free atmosphere. Thus, the height of the ABL and the thickness of the entrainment layer influence radar performance. RAMS resolved sea breeze circulations during the three day cruise that modified the ABL height and entrainment layer resulting in changes to radar performance.

4. ABL STRUCTURE

Figure 5 indicates the location of a ship borne notional radar and the 45 and 225 degree azimuths along which the following meteorological and RF propagation analysis will be performed.

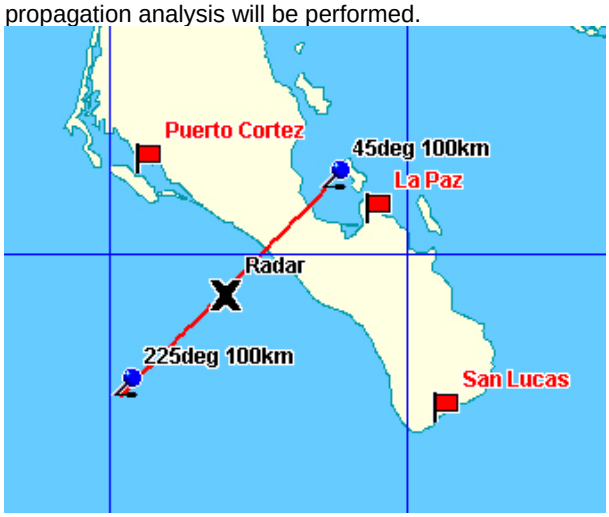

Figure 5: Location of notional radar and azimuths of analysis near the southern end of California Baja Sur.

At 1200UTC (0500 local) on 28 June, 2005, the synoptic flow produced by the seasonal Pacific NW high dominates the surface flow displayed in figure 6.

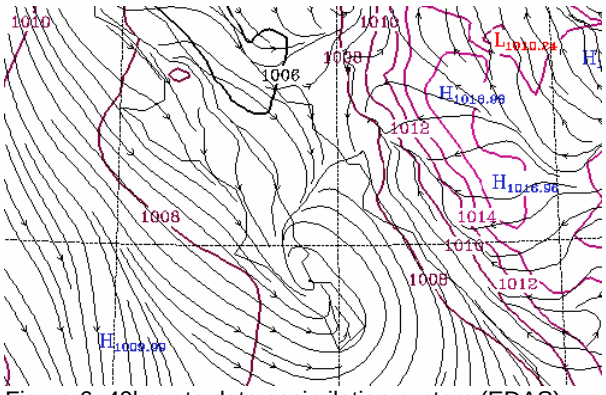

Figure 6: 40km eta data assimilation system (EDAS) with surface streamlines and isobars (mb) at 1200UTC on 28 June, 2005. Image provided by NOAA ARL.

The resulting ABL structure from the ship along a 45 degree bearing can be seen in the θ profiles in figure 7.

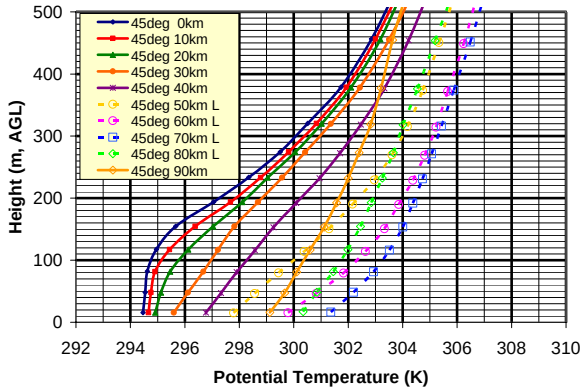

Figure 7: Potential temperature profiles at 1200UTC along a 45 degree bearing from the ship location. The profiles with broken lines are over land.

The ABL is well mixed at the ship but becomes more stable closer and especially over land as would be expected 40 minutes before apparent sunrise. The corresponding profiles for w are displayed in figure 8.

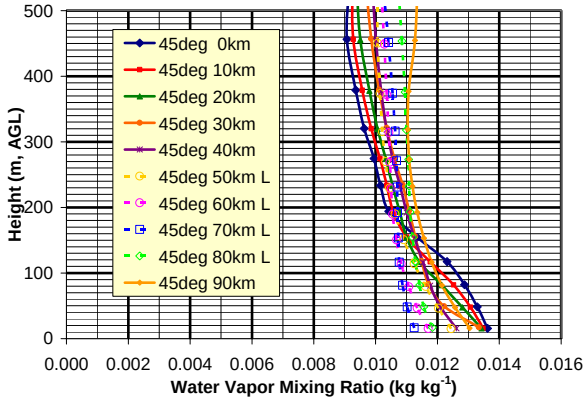

Figure 8: Water vapor mixing ratio profiles at 1200UTC along a 45 degree bearing from the ship location. The profiles with broken lines are over land.

Near surface values of w are greater over the water leading to stronger gradients as the values of w at the top of the ABL are influenced more by the synoptic flow. These gradients in θ and w lead to weak ducting over the water and super refraction over land. This will tend to extend the radar horizon from the ship location along this azimuth beyond that predicted for a standard atmosphere. The resulting profiles of modified refractivity are shown in figure 9.

This change in radar horizon is commonly demonstrated by range height diagrams along an azimuth of the engineering variable propagation factor (PF) measured in the power ratio units of decibels (dB). Propagation factor is defined as the amount of power received from a standard target relative to that received from an atmosphere free of temperature and water vapor gradients. Figure 10 is a plot of PF along the 45

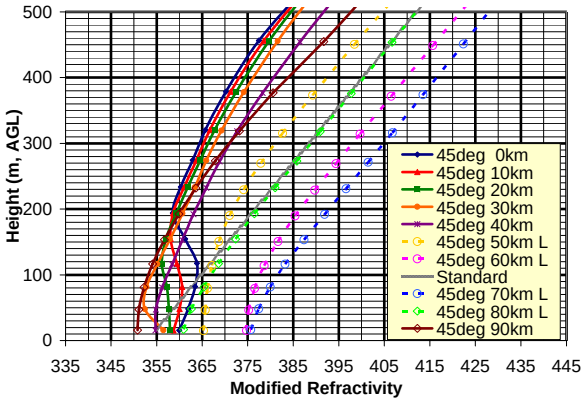

Figure 9: Modified refractivity profiles at 1200UTC along a 45 degree bearing from the ship location. The profiles with broken lines are over land.

degree bearing in figure 5 for a 10cm wavelength radar at the ship location at a height of 22m, ASL. The radar performance is modeled in a standard atmosphere using the Advanced Refractive Effects Prediction System (AREPS, Patterson, 2007).

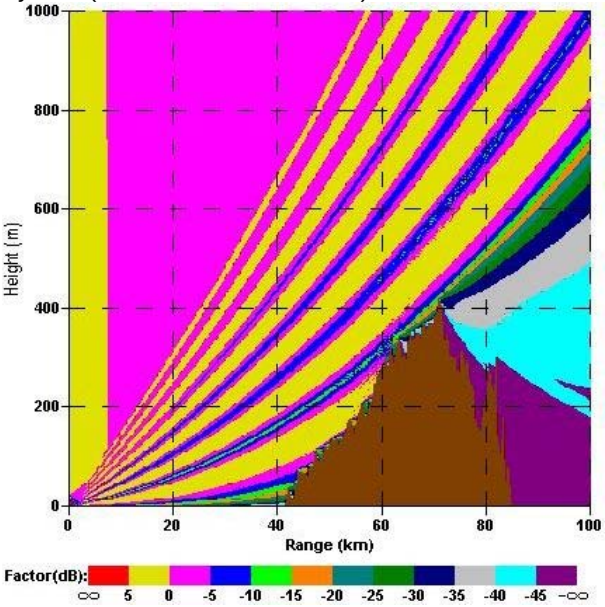

Figure 10: Propagation factor (dB) along the 45 degree bearing in figure 5 for a 10cm radar located 22m, ASL in a standard atmosphere.

The alternating areas of positive and negative PF in height and range are due to electromagnetic energy adding in phase or out of phase as a result of multi-paths from the water surface and directly to a target. The PF decrease in range and height nearer the surface is due primarily to the curvature of the earth. Figure 11 displays PF for the same radar and azimuth but with the atmosphere provided by RAMS in figures 7-9. Notice that the weak ducting and super-refraction tend to bend the energy towards the surface as indicated by the plus 0 to 5dB PF contours near the surface. This is an opportunity to exploit the atmosphere and view low level

threats at a more distant range. On the other hand, the land may provide enhanced clutter that can complicate exploiting the atmosphere. This complication has an engineering solution if the mesoscale NWP data are reliable.

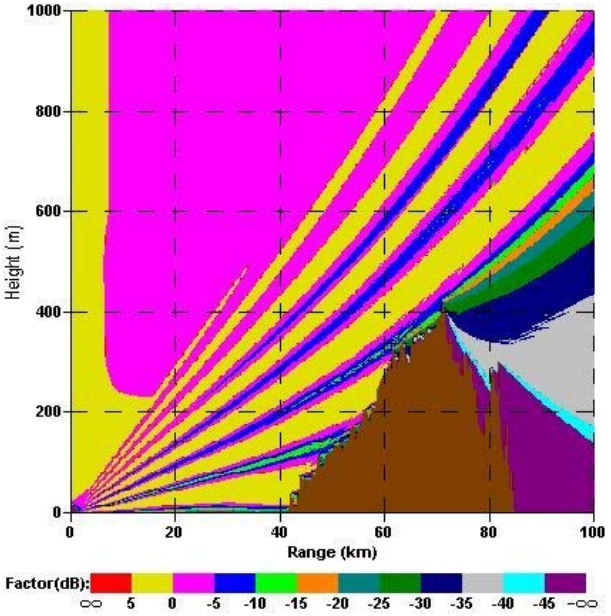

Figure 11: PF plot as in figure 9 but with the RAMS refractivity field at 1200UTC, 28 June, 2005.

By 2000UTC, 30 minutes after solar noon, EDAS has resolved a strong landward flow not only in the Pacific but also in the Gulf of California. This is shown in figure 12.

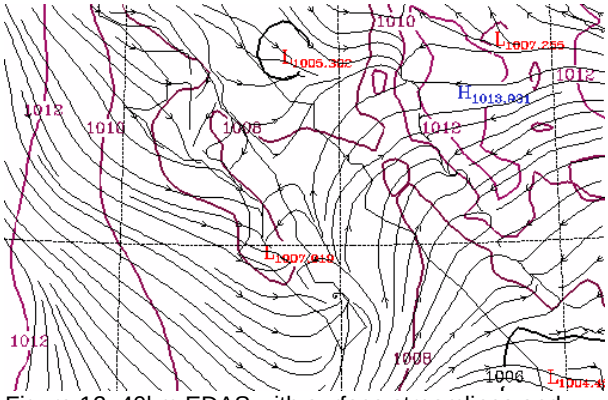

Figure 12: 40km EDAS with surface streamlines and isobars (mb) at 2000UTC on 28 June, 2005. Image provided by NOAA ARL.

RAMS also resolves the sea breeze circulation and the west surface wind along the 45 degree azimuth. The Profiles of θ are shown in figure 13. Over the ocean, the ABL is well mixed, shallower than at 1200UTC, and capped by an entrainment layer. Instability is evident over land near the surface with a deep well mixed layer above.

The corresponding profiles of w are displayed in figure 14. The combination of significantly more water vapor near the surface over water and the lower ABL height combine to produce a weak vertical gradient in w near the surface and an even stronger gradient in the entrainment layer. Water vapor is well mixed over land during this time of day.

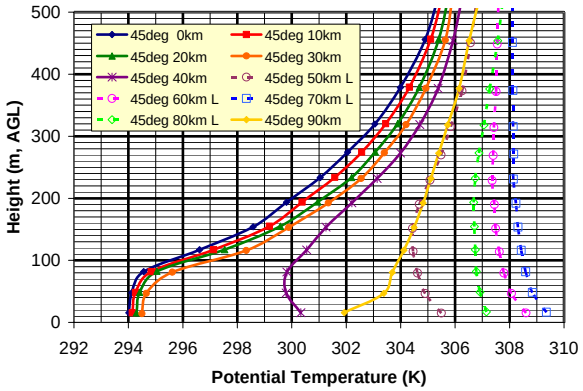

Figure 13: Potential temperature profiles at 2000UTC along a 45 degree bearing from the ship location. The profiles with broken lines are over land.

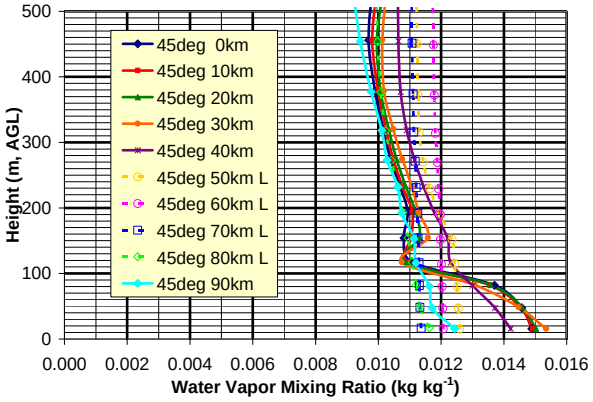

Figure 14: Water vapor mixing ratio profiles at 2000UTC along a 45 degree bearing from the ship location. The profiles with broken lines are over land.

The resulting profiles for M are shown in figure 15. The weaker gradient in w near the surface over the

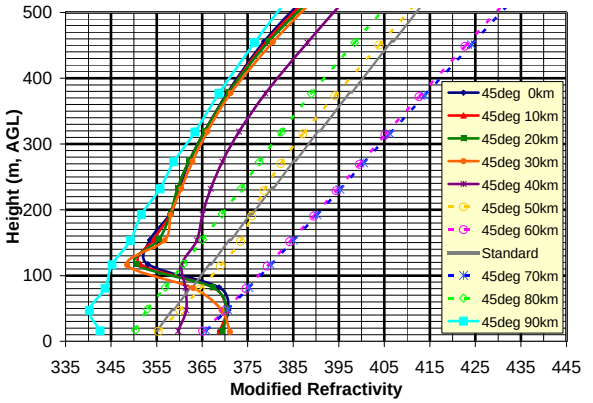

Figure 15: Modified refractivity profiles at 1200UTC along a 45 degree bearing from the ship location. The profiles with broken lines are over land.

water combined with θ being conserved results in super-refraction below the entrainment layer. The thermal stability and increased gradient in w combine to form strong ducting in the entrainment layer. Over land, refractivity in the well mixed layer is in the normal range. The PF range-height diagram in figure 16 demonstrates the resulting impact on a 10cm wavelength radar along the 45 degree azimuth. The greater than 5dB PF contours in red below the entrainment layer are indicative of the ducting. The 0 to 5dB yellow contour near the surface is a result of the near surface super-refraction. These are non standard propagation conditions that can be exploited and can also be detrimental to radar performance.

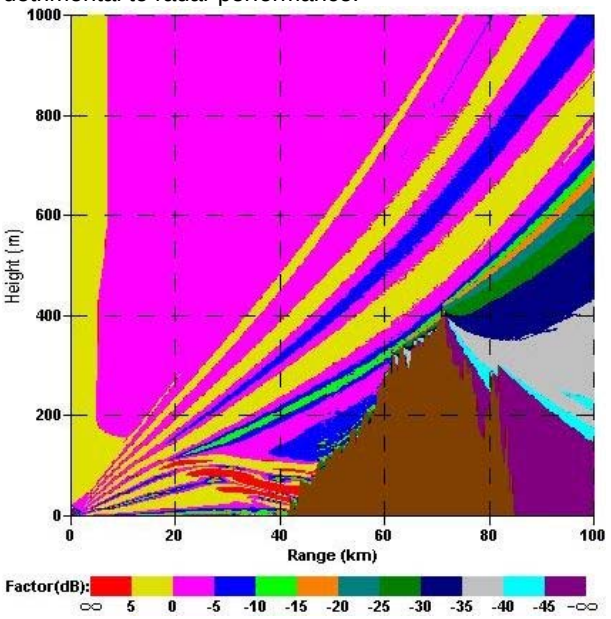

Figure 16: PF plot as in figure 9 but with the RAMS refractivity field at 2000UTC, 28 June, 2005.

A two dimensional method of observing the impact of the ABL on radar system performance is to model the 90% probability of detecting a notional target at a constant height. Figure 17 is derived using AREPS and RAMS to model the 10cm radar capability of detecting a notional target 10mASL at 1200UTC, 28 July, 2005. The yellow range rings are 20km. The white radials indicate the maximum range at which the target can be detected. The red circle delineates the maximum range at which the same target is detectable in a standard atmosphere. It can be seen that the super-refraction shown in figures 9 and 11 increases the detection range looking towards land. By 2000UTC the detectable ranges at 10mASL significantly increase as can be seen in figure 18. The "skip zones" from the SE through the NW are indicative of ducting produced by shallow mixed layers with strong inversions associated with the entrainment layer. This can be observed in the range dependent profiles of M along the 225 degree azimuth in figure 19. The surface wind direction veers from 279 to 303 degrees along this azimuth with range from the radar and ship. The mixed

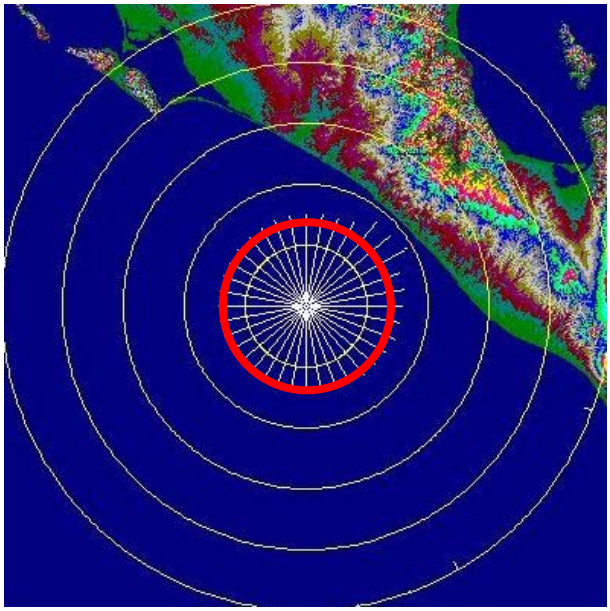

Figure 17: Maximum range with a 90% probability of detecting a notional target at 1200UTC, 28 June, 2005 at 10mASL. Yellow range rings are at 20km. Red contour is the 90% probability of detection in a standard atmosphere.

layer increases with height with distance away from the ship along the 225 degree azimuth during the sea breeze. This is an engineering gift provided by the atmosphere and should be exploited by the radar if the mesoscale NWP data is sufficiently quantitative.

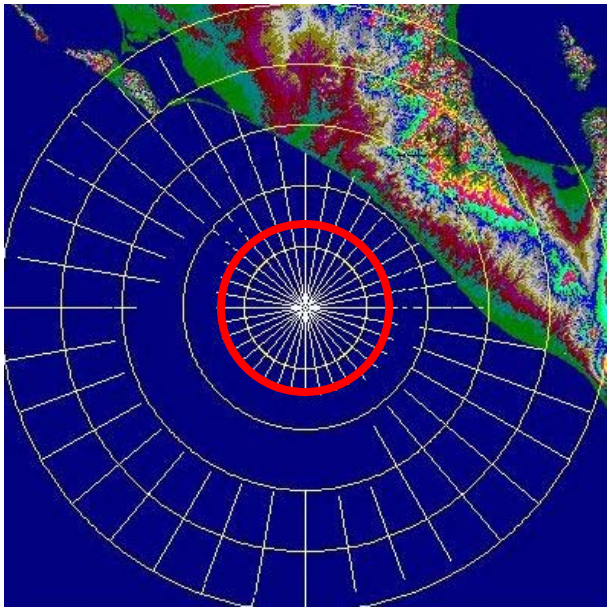

Figure 18: Maximum range with a 90% probability of detecting a notional target at 2000UTC, 28 June, 2005 at 10mASL. Yellow range rings are at 20km. Red contour is the 90% probability of detection in a standard atmosphere.

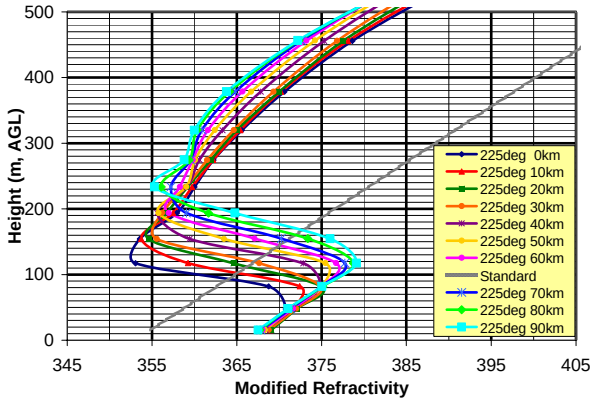

Figure 19: Range dependent modified refractivity along the 225 degree azimuth shown in Fig. 5. at 2000UTC, 28 April, 2005.

The resulting PF plot along this azimuth is shown in figure 20 and illustrates how exploitable RF energy becomes trapped in the ABL. But the spreading cone of -15 to -25dB PF immediately above the range dependent entrainment layer structure is a resulting potential liability.

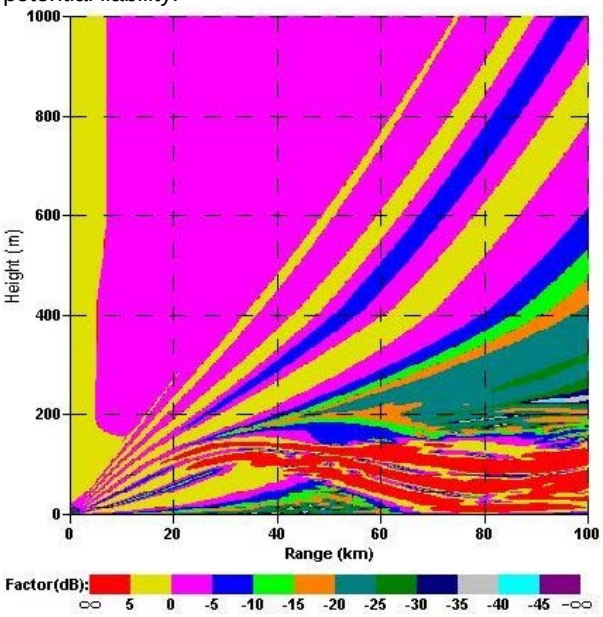

Figure 20: Propagation factor (dB) along the 225 degree bearing in figure 5 for a 10cm radar located 22m, ASL at 2000UTC.

5. CONCUSIONS

Mesoscale NWP resolves the coastal circulations that produce non-standard RF propagation. The RF propagation structure is related to ABL height and thermodynamic profiles that are not always resolved quantitatively. Along the west coast of the US during the seasonal NW Pacific high, it has been observed that the ubiquitous dry air observed in the free atmosphere is not resolved in the global models leading to weaker water vapor gradients in the entrainment layers.

Although the current state of the art for mesoscale NWP as it relates to RF propagation is qualitative, it provides realistic insight into how RF system performance is spatio-temporally impacted by the coastal ABL. Over the water ducting of RF energy is clearly enhanced during sea breeze events as the ABL height decreases and the thermodynamic gradients in the entrainment layer are enhanced. Mesoscale NWP currently provides temperature and water vapor profiles in coastal circulations that are adequately resolved to simulate the performance of prototype radar designs in realistic 4D refractivity fields. The engineering desire is that mesoscale NWP will soon become quantitative to the point that non-standard RF propagation can be exploited in real time by knowledge based radar and communication systems.

6. REFERENCES

Bean, B. R. and E. J. Dutton, 1966, *Radio Meteorology*, National Bureau of Standards Monograph 92

Marshall, R. E. and T. Haack, *Four Dimensional System Engineering Demands on Radar Operating in a Coastal Sub-refractive Environment*, IEEE Radar Conference, Boston, MA, April 17-20, 2007

Marshall, R. E., J Rottier, J. Titlow, and M. Bell, *Radio Frequency Near Surface Anomalous Propagation in the Presence of Diurnal Coastal Air/Sea/Land Interactions*, IEEE/APS/URSI Conference, Albuquerque, NM, July, 2006.

Patterson, W. L., *Advanced Refractive Effects Prediction System (AREPS),* IEEE Radar Conference, Boston, MA, April 17-20, 2007